Dilated and Defunct K Channels in the Absence of K^+

Andrey Loboda, Alexey Melishchuk, and Clay Armstrong
Department of Physiology, University of Pennsylvania School of Medicine, Philadelphia, Pennsylvania, 19104 USA

ABSTRACT Potassium ions are vital for maintaining functionality of K channels. In their absence, many K channel types enter a long-lasting defunct condition characterized by absence of conductance and drastic changes in gating current. We show that channels pass through a dilated condition with altered selectivity as they are becoming defunct. To characterize these abnormalities we examined gating and ionic currents generated by *Shaker* IR and by three nonconducting mutants, W434F, D447N, and Y445A, in 0 K^+. On entering the dilated condition, *Shaker* IR becomes permeable to Na^+ and tetramethylammonium-positive (TMA^+), signaling deformation of the selectivity filter. When dilated, nearly normal closing is possible at −140 mV. At −80 mV, however, closing is very slow and channels stray from the dilated into the defunct condition. Restoration from defunct to dilated condition requires tens of seconds at 0 mV and can occur in the absence of K^+. W434F and D447N are similar to *Shaker* IR, showing Na^+ and TMA^+ permeability when dilated. The defunct gating currents are similar in *Shaker* IR and these two mutants and are reminiscent of the early transitions of normal gating. Y445A does not become defunct and shows Na^+ but not TMA^+ permeability on K^+ removal.

INTRODUCTION

The *Shaker* K channel belongs to a family of voltage-dependent channels that generate potassium-selective currents through membranes upon depolarization. A functional channel is composed of four identical polypeptides with six transmembrane segments in each, S1–S6. The S5 and S6 segments and their connecting link are almost certainly in the center of the channel complex and form a pore that has a narrow filter selective for K^+. S5 and S6 are closely analogous to the two transmembrane crossings of the simple KcsA potassium channel, whose crystal structure is known (Doyle et al., 1998). The selectivity filter of KcsA is composed by the linking region between the two transmembrane segments at the outer end of the pore. The filter is occupied by two or more potassium ions in the crystal structure. The binding sites for K^+ are formed by electronegative backbone carbonyls from the loop that forms the selectivity filter, and the side chains of the filter residues project away from the pore axis. The remainder of the channel is less selective, and its wall is formed by side chains of the residues in S6.

Voltage sensitivity is conferred on *Shaker* by the other four transmembrane segments, in particular the S4 segment, which has seven positively charged amino acids. The KcsA channel, which lacks these segments, is not voltage dependent. Segment S4 moves outward in response to a positive change of the internal potential, driving a conformational change that somehow opens the pore for conduction.

In the absence of permeant ions, potassium channels irreversibly lose the ability to conduct (Chandler and Meves, 1970; Almers and Armstrong, 1980), becoming defunct (Melishchuk et al., 1998). Almers and Armstrong (1980), working on squid axons, suggested that strong, repulsive electrostatic forces develop between negative charges or dipoles in the pore lining when K^+ is removed, destroying the normal conformation of the pore.

Gomez-Lagunas (1997) revisited the effect of 0 K^+ and found that *Shaker* K channels also become defunct on exposure to 0 K^+. Interestingly, he showed that the loss of function does not occur if the membrane is held continuously at −80 mV, preventing the channels from opening. When pulsed open, the channels become defunct at the rate of ~40% per pulse. Apparently, K^+ remains trapped within the channel for as long as several minutes in the closed state. Gomez-Lagunas also showed that channels can be brought back from the defunct condition by restoring K^+ and holding the membrane at 0 mV for tens of seconds.

Another interesting consequence of K^+ removal is the appearance in some potassium channel types of permeability to Na^+ (Korn and Ikeda, 1995). Both *Shaker* IR and the nonconducting W434F mutant become measurably permeable to Na^+ (Starkus et al., 1997, 1998) shortly after K^+ removal.

Gating currents can provide evidence on the conformational states available to a defunct channel. Nonconducting mutants (Perozo et al., 1993; Olcese et al., 1997; Heginbotham et al., 1994) are very useful in this regard because their gating currents can be observed in the presence of K^+ as well as in its absence. The normal gating sequence of *Shaker* consists of multiple transitions, beginning with several early steps in which the subunits are thought to move independently. Later concerted steps may involve cooperative changes among subunits, leading to final opening of the channel (Schoppa and Sigworth, 1998). We show here that all of the nonconducting mutants used in this work are sensitive to K^+ removal, arguing that they retain one or more externally accessible K^+ sites in the selectivity filter;

Received for publication 5 October 2000 and in final form 6 March 2001.
Address reprint requests to Dr. Clay Armstrong, Department of Physiology, University of Pennsylvania School of Medicine, B-400 Richards Building, 3700 Hamilton Walk, Philadelphia, PA 19104. Tel.: 215-898-7816; Fax: 215-573-5851; E-mail: carmstro@mail.med.upenn.edu.

0006-3495/01/06/2704/11 $2.00

and we describe the selectivity and gating changes that occur as channels become defunct.

MATERIALS AND METHODS

Mutagenesis and expression

Mutations were engineered in *Shaker* H4 K^+ channel with the Δ6–46 mutation that removes N-type inactivation (Hoshi et al., 1990). Channels were rendered nonconducting by one of three further mutations: W434F (Perozo et al., 1993), D447N (Olcese et al., 1994), or Y445A (Heginbotham et al., 1994). Mutations were made by polymerase chain reaction between unique restriction sites Xba1/Bgl2 for W434F and Bgl2/Sma1 for D447N and Y445A.

For expression, the channel cDNA was subcloned into the GW1-CMV expression vector (British Biotechnology, Oxford, UK), kindly provided by Dr. Gary Yellen. The mutants were transiently expressed heterologously in tsA201 cells (HEK 293 cells, ATCC CRL 1537, stably transfected with SV40 large T antigen). The channel plasmid (10 μg) was co-transfected with the πH3-CD8 plasmid, kindly provided by Dr. Richard Horn. Cells expressing the CD8 antigen were identified visually by antibody-coated beads. Cells were transfected by electroporation as described previously (Jurman et al., 1994).

Electrophysiology

Ionic and gating currents were recorded in whole-cell configuration 27–72 h after transfection. Membrane potential was controlled using software and hardware made in the laboratory and operated through an IBM PS-2 computer. Currents were recorded using glass pipettes prepared from Kimax-51 capillary tubes (Kimble). Electrode resistance was in the range of 1–2 MOhm. More than 80% of series resistance was compensated. Currents were filtered at 10 KHz and sampled at 20, 50, or 100 kHz. Capacitive and leak currents were subtracted online using a control pulse at very negative (−150 to −200 mV) or positive (100 to 150 mV) potentials. The adequacy of the subtraction protocol was tested by using different starting potentials for the control pulse. The experiments were done at room temperature (20–22°C).

Solutions were made by mixing stock isotonic solutions (290 mOsm). All solutions contained 10 mM HEPES at pH 7.4. The usual extracellular solution contained (in mM) 30 or 0 KCl, 110 or 140 tetramethylammonium chloride (TMACl), 4 $CaCl_2$, 10 HEPES/TMAOH, pH 7.4. These solutions will be referred to in the text as 30 K or 0 K solution. The intracellular solution was (in mM) 20 (*N*-methylglucamine fluoride) (NMGF), 120 NMGCl, 10 HEPES/NMGOH, pH 7.4.

Extracellular solutions containing 140 XCl, 10 HEPES, 4 $CaCl_2$ were also tested, where X was Na^+, $Tris^+$, NMG^+, Cs^+, or Rb^+. The effect of extracellular Ca^{2+} was tested at 0 and 20 mM concentration; extracellular pH at 5.0 and 11; extracellular Ba^{2+} at 4 mM (0 Ca). All the reagents were obtained from Sigma, St. Louis, MO. Solution replacement in the bath can be achieved in seconds by the perfusion system (1 ml/s).

RESULTS

Gating currents

We begin with a comparison of gating in the normal and fully defunct condition and then proceed to the somewhat more complex dilated condition in which the channels show abnormalities in selectivity as well as in gating. Fig. 1 *A* shows normal I_g (gating current) from the nonconducting W434F mutant in 30 K solution, using the pulse protocol shown in Fig. 1 *D*. These records are similar to I_g recorded from *Shaker* IR, if precautions are taken to prevent the channels from becoming defunct when K^+ is removed to eliminate ionic current. A large step to 120 mV drives S4 segments out forcefully and rapidly activates all of the channels, generating I_g ON (gating current as the channels activate) that is large and decays quickly. At the end of the pulse, I_g OFF (gating current as the channels deactivate) is initially near zero, but then rises to a peak, followed by a slow decay. This pattern is seen whenever the channels are fully activated, so I_g OFF transients after large depolarizations (to 0 mV or more) are superimposable. I_g ON, on the other hand, slows progressively from 120 down to 0 mV; as the S4 segments are driven less forcefully, the activation sequence is completed more slowly. Total charge movement as channels activate throughout this voltage range is the same (maximal), and equal but opposite to the charge movement on repolarization. The smallest depolarization, to −80 mV, causes only a small S4 movement, rapidly completed both at the beginning and end of the pulse. Finally, the step to −40 mV causes a slow component in I_g ON, and I_g OFF shows both fast and slow components. Apparently after this step the channels are broadly distributed among the states of the activation sequence. The slow kinetics of I_g OFF after large depolarizations reflect a slow backward rate of the late transitions (see Introduction; Perozo et al., 1993; Schoppa and Sigworth, 1998).

Gating currents from all three mutants are similar in the presence of K^+ and differ mainly in the deactivation rate of I_g OFF after large depolarizations, which is slowest in D447N and fastest in Y445A. Normal currents of the general pattern in Fig. 1 *A* can be recorded from all mutants for at least several hours in the presence of K^+, Rb^+, or Cs^+ either inside or outside.

Gating current changes upon removal of K^+

After removal of K^+ internally and externally, two (D447N and W434F) of the three nonconducting mutants become defunct as judged from their gating currents. The transition from normal to defunct proceeds only with pulsing (Gomez-Lagunas, 1997) and, when the holding potential (HP) is −80 mV, requires roughly 100 gating cycles for W434F but only ~5 for D447N.

The final appearance of defunct I_g, after removing K^+ internally and externally, is shown in Fig. 1, *B* (W434F), *C* (*Shaker* IR), and *D* (D447N). This appearance is stable for hours. I_g ON is reduced in amplitude, and the total charge is decreased by ~30%. Kinetics are also altered. Most noticeably, in the defunct condition kinetics do not change much with voltage, whereas normal I_g ON is faster for a large step than for a smaller one. Alterations of gating current during deactivation are even more obvious. I_g OFF is bigger and faster than normal after large depolarizations, and the rising phase prominent in Fig. 1

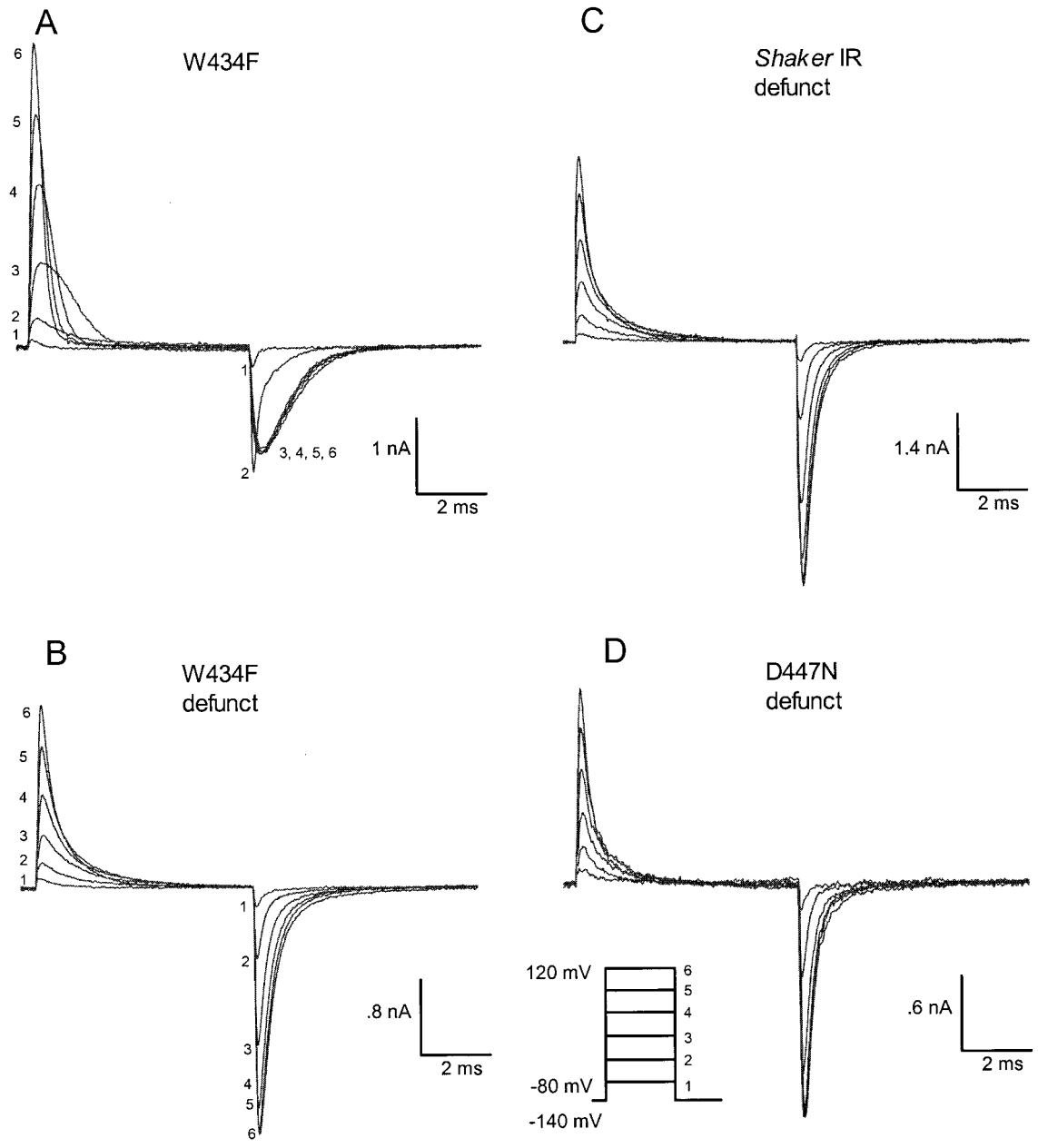

FIGURE 1 Gating currents in the normal and defunct condition. Gating currents were recorded for test voltages between −80 and 120 mV in 40-mV increments (HP = −140 mV) for the channels indicated in the normal (*A*) and defunct (*B–D*) condition. *A* and *B* are from the same cell. *Shaker* IR channels and the nonconducting W434F and D447N mutants have very similar gating currents in the defunct condition. Solutions: (*A*) 30 K solution; (*B–D*) 0 K solution.

A is absent. The dramatic slow-down associated with channel opening is lost because channels do not reach the open state, from which the return is slow. As a result, all of the I_g OFF traces are fairly similar in time course. After small depolarizations the kinetics and voltage dependence of I_g OFF in the defunct state are similar to normal I_g OFF. Once defunct, gating currents are quite similar for the nonconducting mutants illustrated and for *Shaker* IR channels (Fig. 1, *B–D*).

The effect of the defunct condition on total gating charge movement is shown in Fig. 2, where the *Q-V* (charge-voltage) plots are normalized relative to Q_{tot}, the total charge movement for a large depolarization in normal conditions (presence of external K^+). The normal *Q-V* curves of the three nonconducting mutants are very similar. Y445A does not become defunct (cf. Fig. 6) and retains its normal *Q-V* curve in 0 K solution. The other two nonconducting mutants and *Shaker* IR have, when

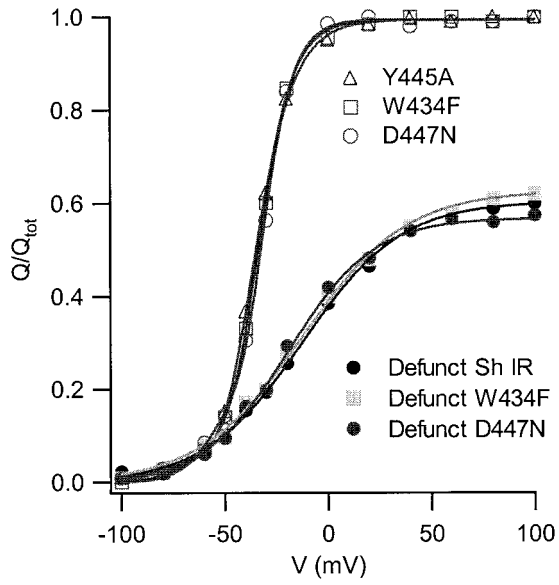

FIGURE 2 The *Q-V* curve in the defunct condition is altered, presumably because the late steps in gating are abolished. *Q* was measured from the area under the I_g OFF transient. *Q-V* plots of three nonconducting mutants D447N, Y445A, and W434F are shown in the presence of potassium by the upper curves. The lower curves are for *Shaker* IR, W434F, and D447N in the defunct condition.

defunct, very similar *Q-V* curves as well as gating currents (Fig. 1). Maximum *Q* at high voltage is about two thirds of normal, and the curves spread over a broader voltage range.

A dilated condition is visited on the path to the defunct condition

After removal of K^+, those mutant channels that become defunct in Figs. 1 and 2 transiently show abnormal permeability, making it clear that their selectivity filters are deformed. Soon after K^+ removal, I_g ON in these mutants is approximately normal, but the channels become measurably permeable to Na^+ (Starkus et al., 1997). To our surprise these mutants also have a measurable permeability to TMA^+ and other large cations at this time. Some characteristics of this current are shown in Fig. 3, *A* and *B*, and current carriers are identified in Fig. 3 *C*. Fig. 3, *A* and *B*, show the transition from normal to a dilated, large-cation-permeable condition and finally to the defunct condition. The traces were taken in the order indicated by the numerals, and the holding potential was −80 mV. Trace 1 shows the normal gating current, typical of W434F, in 30 K solution. I_g OFF is slow and has a prominent rising phase. Trace 2 was recorded after a short time in 0 K solution, when some of the channels were fully defunct, some were in the dilated condition, and some still normal. I_g ON is reduced, but the most notable changes are in the tail upon repolarization. First there is a quick spike of I_g OFF, generated by defunct channels (cf. Fig. 1 *B*), followed by a very slow phase that continues long after the end of the trace. Total charge movement in the tail of trace 2 is 25 times larger than in the ON transient of the same trace, indicating the presence of an ionic component in the tail. The ionic component could be blocked by re-immersing the cell in 30 K solution (trace 3). This changed neither I_g ON nor the early spike of I_g OFF in the tail, but eliminated most of the ionic current responsible for the very slow phase. In trace 3, the ratio of OFF to ON charge movement is 1.15, indicating that most of the ionic component is blocked by K^+. Trace 3, then, is mainly a mixture of I_g generated by normally gating channels (the slow component after the notch) and a small fraction of defunct channels (the initial spike).

After recovery in 30 K solution at 0 mV, followed by restoration of the holding potential to −80 mV, trace 4 was recorded: normal I_g, similar to trace 1 but somewhat smaller presumably because of rundown. A long soak in 0 K solution then reduced I_g ON by ~60% and caused a large early spike to appear in the tail current (trace 5). The ionic component in the tail is now quite small as can be seen from the small difference between traces 5 and 6, the latter in 30 K solution to block the ionic component. In summary, as the channels become defunct, I_g ON gets smaller, falling to ~40% of normal (at this *V*), and most of the tail gating current is compressed into a fast spike (trace 6; cf. Fig. 1 *B*). The ionic component that appears quickly on immersion in 0 K^+ disappears as channels progress from dilated to defunct. The rounded tail generated by normally gating channels is absent.

Large cations carry current through dilated channels

There is no obvious candidate for the current carrier in the ionic conditions used in Fig. 3, *A* and *B*, where both Na^+ and K^+ are absent. The same current can be elicited by holding at 0 mV and stepping to −150 mV, as shown in Fig. 3 *C*, *trace a*; holding at 0 mV was found to maintain the channels stably in a dilated condition as shown below, and for this reason HP = 0 mV in this and most of the following figures. Note that the ionic current is initially zero and develops over the course of ~10 ms as the dilated channels pass from a nonconducting to a conducting state at −150 mV (see below). When 70% of the TMACl in the extracellular solution was substituted with glucose (Fig. 3 *C*, *trace b*), the area under the tail current reversibly (*trace c*) decreased to about one-fourth without changing I_g ON. The current is only slightly reduced by changing from TMA^+ to NMG^+ or $Tris^+$ (not shown), showing that extracellular cations as large as NMG^+ and $Tris^+$ permeate through dilated channels in their conducting state. The ionic tail current is unaffected by pH 9 and by removing Ca^{2+}, suggesting that neither Ca^{2+} nor H^+ are current carriers.

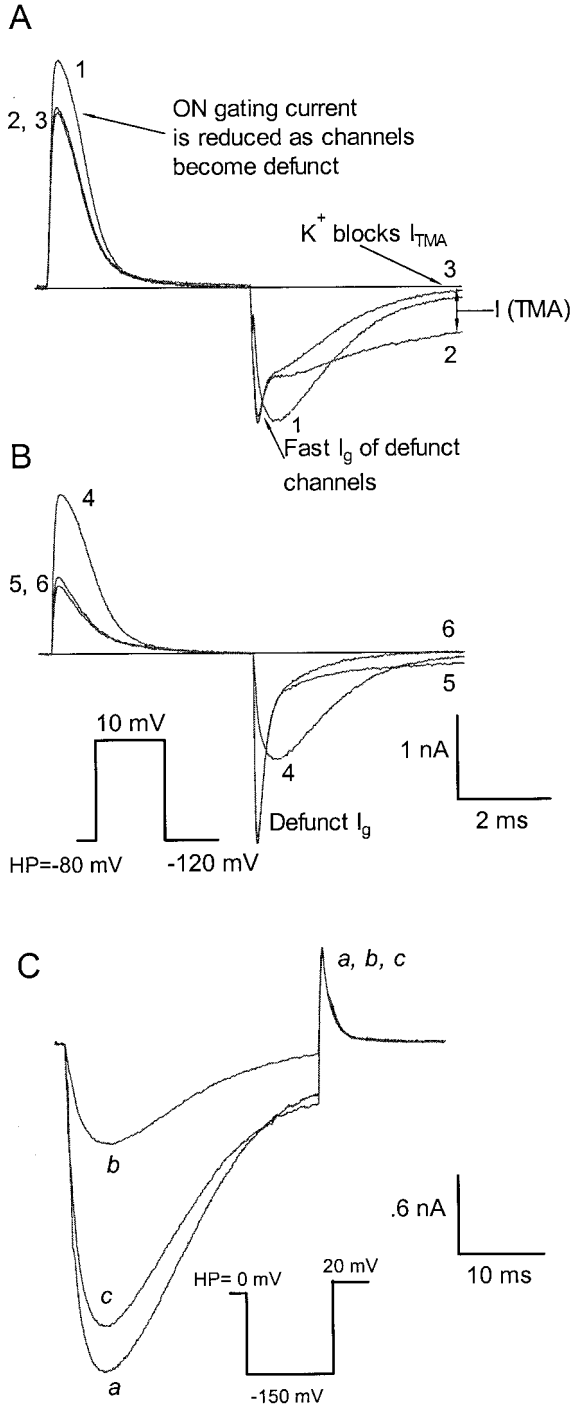

FIGURE 3 An ionic component appears in the tail in 0 K solution. (*A* and *B*) Normal gating currents of W434F in 30 K solution (*traces 1* and *4*), the results of short (*trace 2*) and long (*trace 5*) exposure to 0 K solution (recorded in 0 K solution), and the currents after quick restoration of 30 K solution (*traces 3* and *6*). The ionic tail current can be quickly blocked by restoration of K^+. (*A*) In trace 2, a small fraction of the channels are defunct, making I_g ON 15% smaller than normal (*trace 1*). The fast spike in the tail of traces 2 and 3 is generated by the defunct channels. In trace 2 the spike is followed by a mixture of I_g (similar in time course to *trace 1*) and ionic current carried by TMA^+. In trace 3 the ionic component has been blocked by restoration of 30 mM KCl. (*B*) Almost all channels are defunct. I_g ON is reduced by 60%. I_g OFF is mainly fast, and there is little TMA^+ current to be blocked by K^+ addition (*trace 6*). (*C*) The ionic composition of the extracellular solution was changed from TMACl (*trace a*) to 30% TMACl 70% Glucose (*trace b*) and back to TMACl (*trace c*). Substituting TMACl with glucose causes an 80% reduction in the ionic current without appreciable change in I_g ON, arguing that TMA^+ carries the ionic current in the tails. HP = 0 mV.

Large-cation permeability was observed only in mutants that were subject to becoming defunct; i.e., all except Y445A (see below).

Channels can recover from the defunct to the dilated condition without K^+

It is known that holding at 0 mV in the presence of K^+ allows channels to recover from the defunct to the normal condition (Gomez-Lagunas, 1997). We find that holding at 0 mV for more than 30 s, even in the absence of K^+, is sufficient to restore defunct channels to the dilated (though not the normal) condition, in which characteristic large-cation permeability can be demonstrated by strong hyperpolarization. Shown in Fig. 4 *A* are three current traces from *Shaker* IR channels in 0 K solution. The protocol (see inset) was identical in all three cases, but the histories before it was applied were different. Beginning with events at −150 mV (HP = 0 mV), none of the channels had been allowed to become defunct before trace i. Consequently, the step to −150 mV elicits a large-cation tail current. The channels were then made defunct by 10 steps to −80 mV for 500 ms from 0 mV (not shown), and while most channels were still defunct, trace ii was recorded. There is a fast initial spike of I_g OFF that is characteristic of defunct channels, and the ionic component in the tail is almost absent. After trace ii, holding for 2 min at 0 mV restored the ionic current in the tail on stepping to −150 mV (trace iii); evidently, the channels recovered from the defunct to the dilated condition.

After channels in the dilated condition have been closed by a step to −150 mV, they generate gating currents of almost normal appearance on stepping to 20 mV (Fig. 4 *A*, *traces i* and *iii*), whereas trace ii has the reduced and more rapid I_g ON seen with defunct channels. I_g ON generated by dilated channels after closing at −160 mV is shown at numerous voltages in the inset of Fig. 4 *B*. This family of traces resembles the normal family shown in Fig. 1 *A*. In particular, the time course at +40 mV is much faster than at −40 mV, and the +40- and −40-mV traces cross. Comparing the *Q-V* curve of these currents (Fig. 4 *B*, closed circles) to those of W434F in 30 K solution (open circles), it is normal in shape and steepness, but left-shifted by ~10 mV. This shows that dilated channels pulsed to −160 mV enter almost normal closed states.

To further examine the gating status of the channels during a tail at very negative voltage, the pulse was inter-

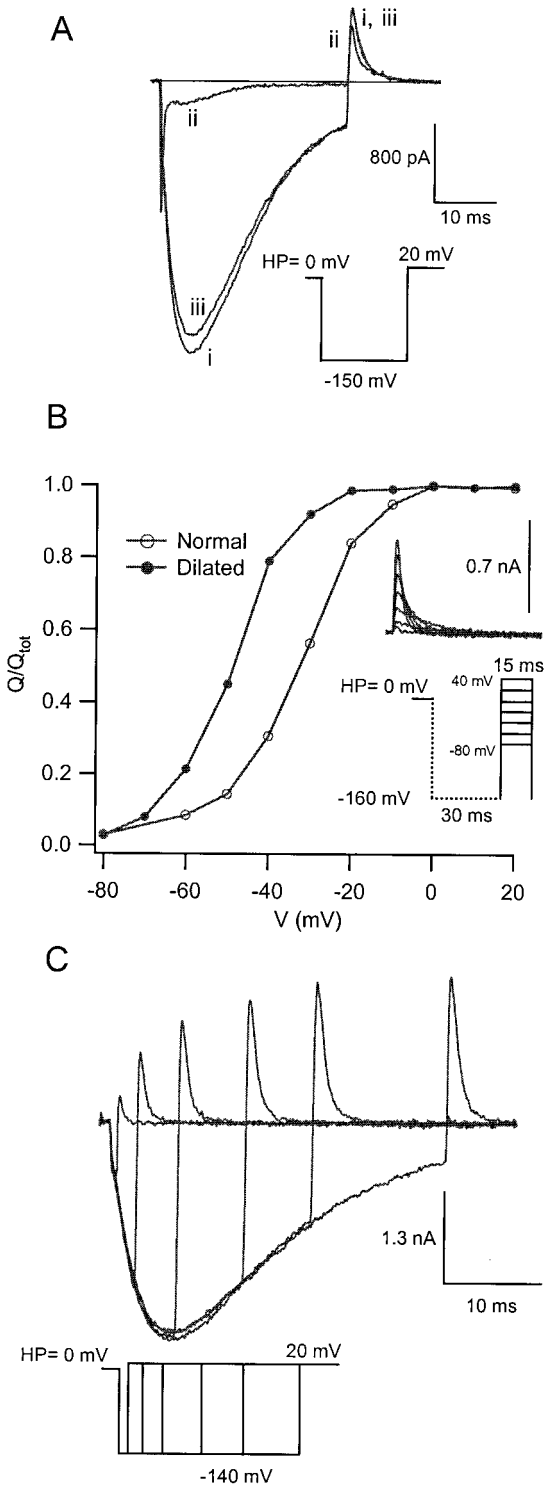

FIGURE 4 The dilated condition, characterized by a slow ionic tail current as seen in Fig. 3, is stable at 0 mV. (*A*) Recovery of channels from defunct to dilated in 0 K^+ at a holding potential of 0 mV. In trace i, a slow large-cation tail current is elicited by a pulse to −150 mV from HP = 0 mV (dekalified *Shaker* IR channels in 0 K^+ TMACl//NMGCl). A repolarization to 20 mV elicits I_g ON of normal configuration. Trace ii was elicited from channels made defunct by ten 500-ms pulses to −80 mV. Defunct channels have fast I_g OFF and reduced I_g ON and do not conduct. Finally, after a 120-s hold at 0 mV to recover channels from defunct to dilated, trace iii was recorded. (*B*) *Q-V* curves of normal (W434F in 30 K solution) and dilated channels. The curves are similar but displaced along the voltage axis. The inset shows I_g ON from the dilated channels. (*C*) The return of gating charge to rest position was studied by applying pulses of different duration to −140 mV and testing with a return to +20 mV. I_g ON elicited by the step to +20 mV increases in amplitude with duration of the hyperpolarizing pulse but has the same time course throughout.

rupted at various points by stepping to +20 mV and recording gating current (Fig. 4 *C*). I_g ON is quite small when the interruption is early (most of the channels are still dilated and nonconducting) but has a time course, when scaled up, that is indistinguishable from normal (i.e., W434F in 30 K solution). We take the amplitude of I_g ON as a measure of the channels that have returned to a near normal closed state. The amplitude increases steadily as channels move from dilated nonconducting to dilated conducting to closed. Interestingly, repeated steps to −140 mV made none of the channels defunct as can be seen from the unvarying size of the current tails. The different consequences of stepping to −80 mV versus more negative values are examined in more detail in Figs. 7 and 8.

This complex set of phenomena can be summarized as follows. 1) In the absence of K^+, channels indefinitely reside in a dilated, nonconducting state at 0 mV. 2) Stepping repeatedly to −80 mV makes the channels defunct. 3) Stepping to −140 mV or more negative causes the dilated nonconducting channels to enter a dilated conducting state within ~10 ms, and in this state they are permeable to large cations e.g., TMA^+, NMG^+, and $Tris^+$. 4) After ~30 ms at −140 mV the channels enter closed states that are almost normal, as judged by I_g ON on subsequent depolarization.

Voltage-dependent closing kinetics of dilated channels

The kinetics of the nonselective current provide clues to the gating behavior of channels in the dilated condition. A family of tail currents elicited by hyperpolarizing pulses from HP = 0 mV (similar to the procedure of Fig. 4) are shown in Fig. 5 *A*. No ionic current at all is seen at voltages less negative than −80 mV (not shown). At −80 mV ionic tail current is quite small, and as demonstrated in Fig. 7, the channels slowly become defunct at this voltage. At more negative voltages the tails become progressively larger and faster both in their rise to peak and in their decay. As noted above, all the tail currents have a rising phase, which indicates that the dilated channels are nonconducting at 0 mV. (The quick initial spike in some traces is generated by a small fraction of defunct channels.) They enter the conducting condition within ~5–15 ms depending on V_m and then close within 20–50 ms. Almost identical currents can be obtained for the D447N mutant (Fig. 5 *B*), which has a

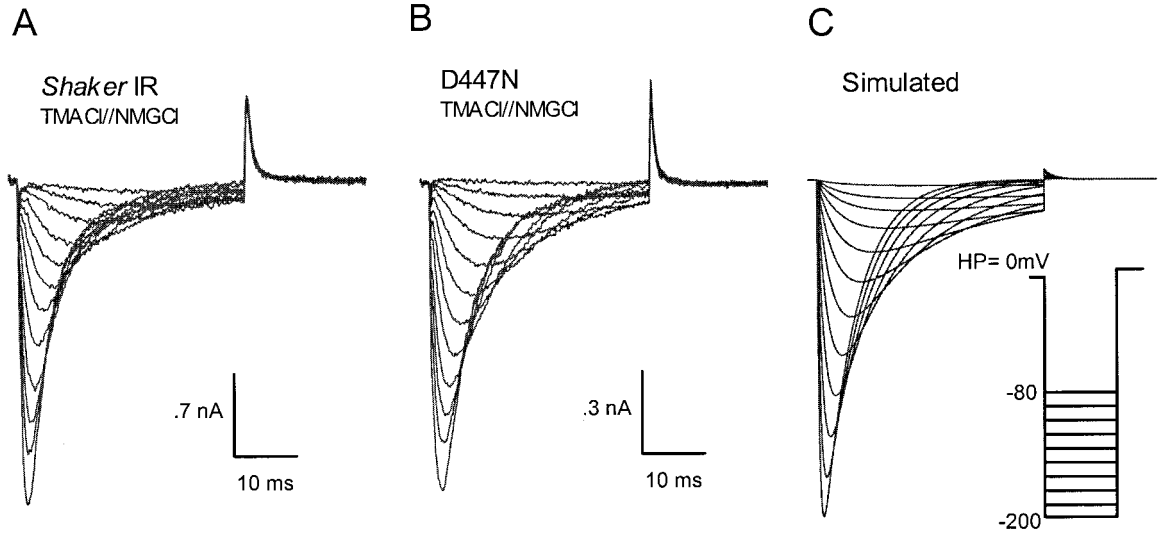

FIGURE 5 Kinetics and voltage dependence of the large-cation current. (*A* and *B*) TMA^+ currents were elicited by hyperpolarizing pulses from −80 to −200 mV (see pulse diagram; 0 K solution). Current was near zero for pulses less negative than −80 mV. (*A*) *Shaker* IR; (*B*) D447N; (*C*) Large-cation currents are simulated using the model given in the Discussion.

similar rate of becoming defunct. Fig. 5 *C* is a simulation of Fig. 5, *A* and *B*, and is described in the Discussion.

Y445A in 0 K^+ is Na^+ but not TMA^+ permeable

Some mutant *Shaker* channels do not become defunct in 0 K^+ (Melishchuk et al., 1998), although they demonstrate measurable sodium conductance. Fig. 6 shows currents of the nonconducting mutant Y445A elicited from HP = 0 by the same voltage protocol as in Fig. 5. Y445A does not become defunct under any conditions we have found (see Fig. 2). After K^+ removal, a sizable sodium current develops (Fig. 6 *A*). This current does not change with time; i.e., the channel never becomes defunct. The ionic current disappears when Na^+ is replaced by TMA^+ (Fig. 6 *B*), showing that the channel is not TMA^+ permeable. This is quite different from the behavior of *Shaker*, W434F, and D447N, which show a large TMA^+ current (Fig. 5). Gating behavior is also much different: at any given voltage, the tail kinetics are much faster than in Fig. 5.

Kinetics and voltage dependence of becoming defunct

As noted above, channels become defunct at −80 mV but enter almost normal closed states at −160 mV. We measured the rate of becoming defunct, using the two-pulse protocol shown in Fig. 7 *A*. After a 1-min hold at 0 mV (the extreme left of the protocol) all channels are in the dilated condition and capable of carrying TMA^+ current when V_m is stepped to −160 mV (trace 1, first pulse to −160 mV). Traces 2–6 (for which the first pulse is to −80 mV) show that there is essentially no TMA^+ current at −80 mV (cf. Fig. 5). After an unsampled interval τ_n of varied duration at −80 mV, V_m was stepped to +40 mV for 10 ms to activate the channels. (The 10-ms step was unsampled, but Fig. 4 shows I_g ON generated by a similar protocol.) This step is long enough to fully activate closed, dilated channels but too short to recover channels from the defunct condition. Thus, channels made defunct in the first pulse are still defunct in the test (second) pulse to −160 mV and do not contribute TMA^+ current. A 35-ms interval at −80 mV (Fig. 7 *A*, *trace 2*) makes 10% of the channels defunct, as judged from the amplitude of the ionic current in the test pulse. As the duration of the interval at −80 mV increases (Fig. 7 *A*, *traces 3-6*), more and more channels become defunct, reaching 80% for a 1-s interval. The defunct fraction of the channels as a function of the interval at −80 mV is shown in the graph in Fig. 7 *B*. Most of the channels become defunct, and few, if any, close normally at −80 mV.

The voltage dependence of closing versus becoming defunct was studied in Fig. 8, using the protocol illustrated. The channels are mainly in the dilated condition after a 1-min hold at 0 mV (extreme left of protocol). A 50-ms conditioning step to the indicated voltage was applied, followed by a 500-ms interval at −80 mV, an activating step to +40 mV, and a test step to −160 mV (cf. Fig. 7). The results show that a very negative conditioning step, e.g., to −200 mV, puts most of the channels into the closed state, where most of them remain during the interval (500 ms) at −80 mV, allowing them to contribute to the ionic current in the test step; trace h, at −160 mV, is almost as large as trace f during the first pulse, which was also to −160 mV. In contrast, less negative steps do not cause closing. Instead channels that have not been forced to close by a very

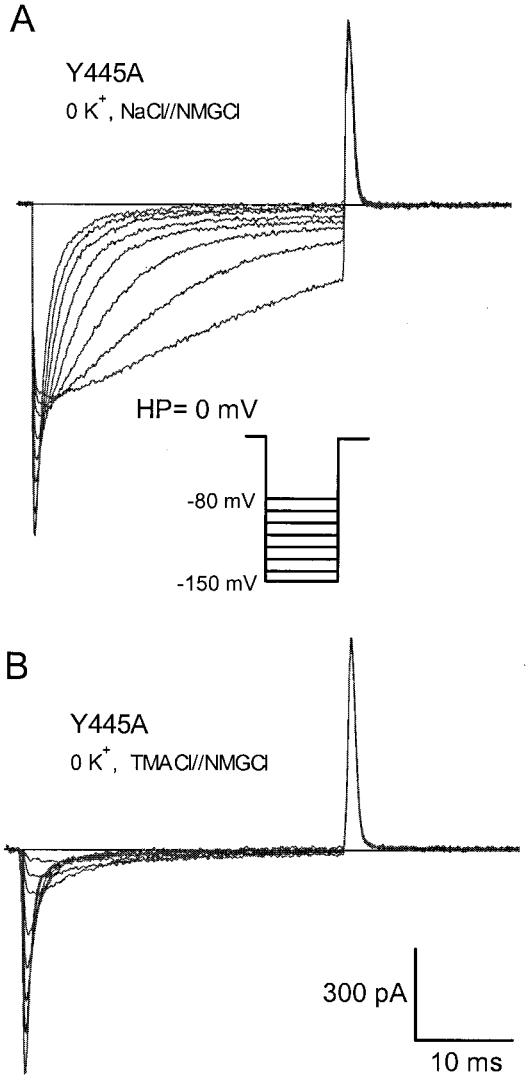

FIGURE 6 Y445A in 0 K solution does not become defunct and is permeable to Na^+ but not to TMA^+. (*A*) There is substantial ionic current through Y445A channels in 0 K^+ when Na^+ is present. (*B*) The ionic component disappears in 0 K^+ when Na^+ is replaced by TMA^+, leaving only gating current.

negative step become defunct during the 500-ms interval at −80 mV, thus reducing the current in the test step. The fraction that is defunct as a function of voltage in the conditioning step is shown in the graph in Fig. 8 *B*. The *y* axis shows the defunct fraction in the second step, using trace f during the conditioning pulse (−160 mV) for normalization. The curve rises only to 0.6 because the interval at −80 mV is not long enough to make all channels defunct (see Fig. 7). Positive to −80 mV the curve turns down, and as shown above (cf. Gomez-Lagunas, 1997), none of the channels are defunct after a long hold at 0 mV.

In summary, channels slowly become defunct at −80 mV (Fig. 7). A strong negative pulse forces the channels into almost normal closed states and prevents them from becoming defunct (Fig. 8).

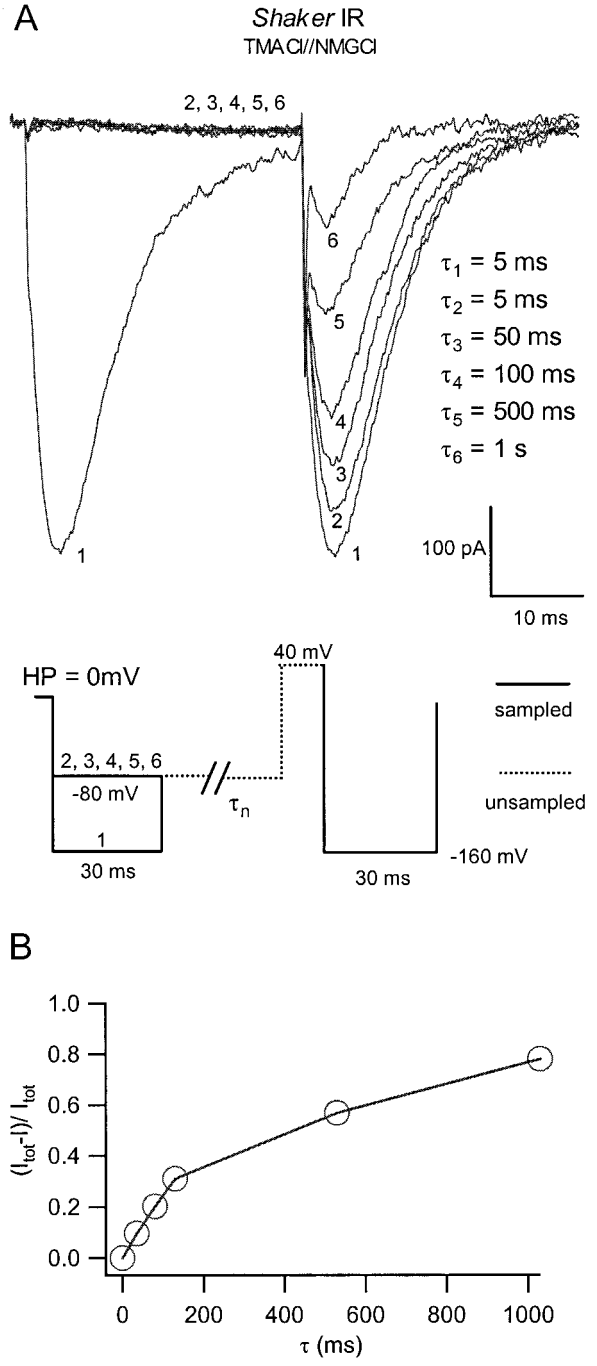

FIGURE 7 Channels become defunct slowly at −80 mV. The absence of ionic current in the defunct condition was used to measure the proportion of defunct channels. (*A*) Large-cation currents recorded with voltage protocols that consist of a conditioning period, a reactivating step (40 mV/10 ms), and a test pulse (−160 mV/30 ms). Trace 1: the conditioning period is a step to −160 mV/30 ms, followed by a 5-ms interval at −80 mV. The first step, to −160 mV, closes the channels, preventing them from becoming defunct, resulting in a large current during the test step (*trace 1*). For traces 2–6 the conditioning period is a step to −80 mV for 5–1000 ms. This makes progressively more channels defunct, reducing ionic current in the test step. After each trace, channels were held at 0 mV for 1 min to recover them from the defunct condition. (*B*) The fraction of channels made defunct by the conditioning period at −80 mV is plotted as a function of the interval at that voltage. I_{tot} is the peak current in trace 1.

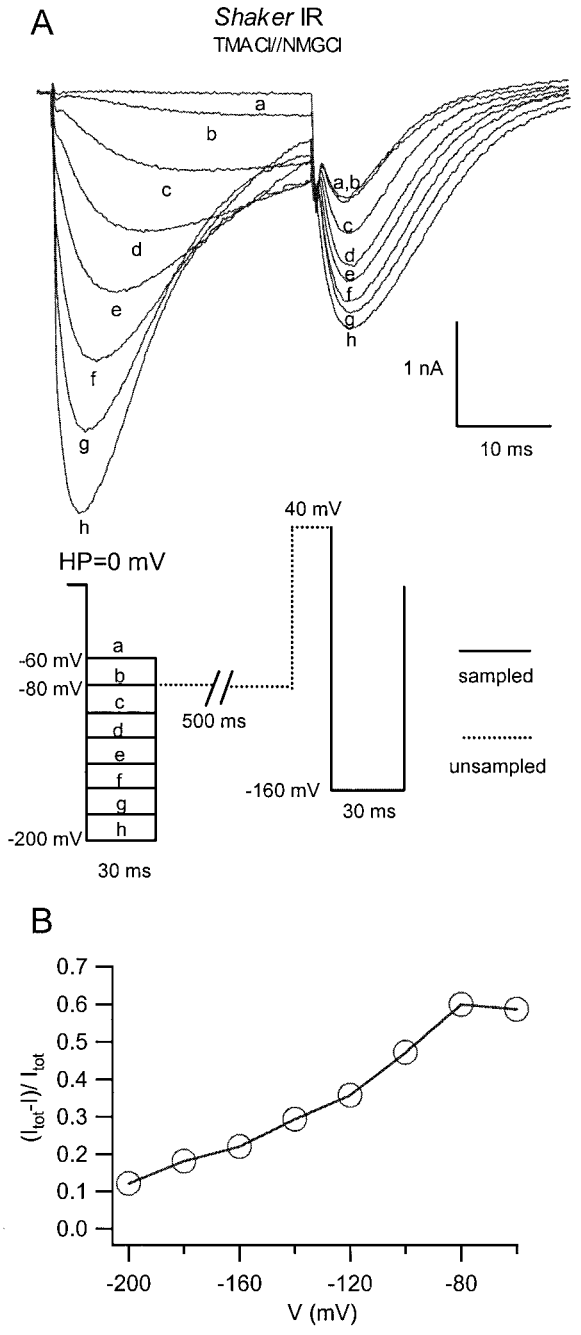

FIGURE 8 The effect of V_m during a conditioning step on the percentage of channels made defunct. (*A*) The first step (−60 through −200 mV) closes a fraction of the channels, progressively more as V_m is made more negative. A 500-ms interval (unsampled) at −80 mV then makes defunct most of the channels that were not closed by the first step. The channels are then reactivated by a step to 40 mV (unsampled) and tested by a step to −160 mV. Hyperpolarized V_m in the conditioning step closes channels, preventing them from becoming defunct. (*B*) The defunct fraction of channels is plotted as a function of V_m during the conditioning step.

DISCUSSION

This paper continues the study of the defunct condition of K channels resulting from total removal of K^+ on both sides of the membrane (Gomez-Lagunas, 1997; Melishchuk et al., 1998). The most important findings are the following.

1) Two nonconducting mutants of *Shaker* channels, as well as *Shaker* IR, require potassium ions in the pore for normal gating and become defunct in 0 K^+. As judged from gating currents, the defunct condition is similar for both conducting *Shaker* IR and these two nonconducting mutants. Y445A, another nonconducting mutant, does not become defunct.

2) In the defunct condition the total gating charge is decreased by a third at high voltage. The missing charge is approximately the same as the charge carried by the late steps in activation gating, as measured elsewhere (see Introduction).

3) An ionic current, carried by large cations like NMG^+ or TMA^+, is found after K^+ removal in channels that can become defunct (*Shaker*, W434F, and D447N) but not in Y445A, which cannot. The large size of the permeating ions argues that the pore of dekalified channels is dilated, supporting the hypothesis of Almers and Armstrong (1980) that electronegative groups in the pore repel each other in the absence of a resident cation.

4) The large-cation current can be elicited only by hyperpolarizations more negative than −80 mV. The exceptionally slow closing kinetics of this current suggest that the backward rates of the late concerted steps in the activation sequence are 100 times slower than in potassium-occupied channels. The abnormal selectivity filter apparently makes normal closing of the channels extremely slow and energetically unfavorable (cf. Heginbotham et al., 1994). At strongly hyperpolarized potentials (−140 to −200 mV), the voltage sensor can push the channels into almost normal closed states, but at less negative potentials (−80 mV) the channel becomes defunct.

To examine the gating abnormalities that result from removing K^+, we used several nonconducting mutants with alterations in the pore region. These mutants retain normal gating as judged from the similarity of their gating currents to *Shaker*. Measurement of gating current in *Shaker* is difficult because the channels become defunct within a short time unless a cation that permeates reasonably well through K channels is present on at least one side of the membrane. Use of the nonconducting mutants allows measurement of I_g in the presence of K^+. Two of the three mutants become defunct when K^+ is withdrawn.

Where in the channels are the essential K^+ ions located? The thorough wash required to cause gating changes argues that the crucial binding sites have a high K^+ affinity. These sites, perhaps more than one per channel, hold the last K^+ ion(s) in the pore, presumably in the selectivity filter, keeping the channels from becoming defunct. Ba^{2+} binds to the innermost site in the selectivity filter (Jiang and MacKinnon, 2000) and can prevent the W434F mutant from becoming defunct in the absence of K^+ (Gomez-Lagunas,

1997; our observations). Thus, the inner site is apparently intact and externally accessible in nonconducting mutants, implying that the lesion in W434F that destroys its conductance is a subtle alteration of the outer site. This intimates that K^+ occupancy of the inner site is crucial to maintain normal gating in W434F.

What is the nature of the changes that occur in the P region when K^+ is removed? As suggested years ago, the results are consistent with the idea that the pore dilates as a consequence of having no counter-cations for the electronegative carbonyls that line the selectivity filter. An early stage of this dilatation may be the Na^+ permeability that appears after K^+ removal. Some channels, e.g., Y445A (above) and T449V (Melishchuk et al., 1998) do not progress beyond this stage. Others, e.g., *Shaker* (conducting) and W434F and D447N (both nonconducting), progress to the dilated condition in which large cations can permeate.

How is the change in the P region transmitted to the remainder of the channel? There is precedent for P region changes (by mutation) that cause gating changes. Heginbotham et al. (1994) found that many P-region mutants have altered gating. In particular, in their work all of the channels that became nonselective as a result of a mutation deactivated with slow kinetics, regardless of the position of the mutation. The link between changes in selectivity and gating remains to be determined. Here we have shown that channels in the dilated condition have very slow closing kinetics. Modeling of the nonselective current (Fig. 5) and comparing its rates with the late steps in the normal gating sequence (Schoppa and Sigworth, 1998) show that the backward rates of the late transitions are 100-fold slower in channels in the dilated condition (rates are given below). The late transitions reflect closing of the gate and probably involve conformational changes in the pore domain. Slow backward rates of the late transitions in the dilated condition suggest that changes in the selectivity filter make closing of the channel unfavorable. As judged by the slow return of the gating charge upon hyperpolarization from 0 mV (Fig. 4 *C*), the voltage sensor must wait until the gate is closed to return to its resting position at negative potentials. When V_m is changed from 0 to −80 mV, the S4 helices of channels in the dilated condition sense the change in potential but are unable to press the gate to close normally. Instead the channel enters the defunct condition. At −140 mV the drive on the S4 helices is sufficient to force the gate to close normally despite the abnormalities in the selectivity filter caused by the absence of K^+.

There are two general possibilities for the absence of conductance in the defunct condition: either the selectivity filter is permanently collapsed, or the intracellular gate is closed. Two lines of reasoning suggest that the latter idea is preferable. First, TMA^+ permeability shows that the pore dilates rather than collapses. Second, the fact that polarization to −80 mV is necessary to make the channel defunct suggests that the S4s move inward, driving the gate into an abnormal (defunct) position. Thus, of the two possibilities mentioned, we favor the idea that a gating abnormality of a channel with an abnormally distended selectivity filter underlies the absence of conductance.

In the defunct condition the channel is closed abnormally but retains considerable gating charge movement. Compared with normal gating several important features of defunct gating stand out. 1) The *Q-V* curve is shallow and saturates near 50 mV, whereas the normal *Q-V* saturates at ~−30 mV. 2) The maximum gating charge in the defunct condition is 30% percent less than normal. 3) Defunct tail gating currents are fast after depolarizations of all sizes, and their kinetics and voltage dependence are similar to the normal tails after small depolarizations. Facts 2 and 3 suggest that a semblance of the normal early transitions occurs in the defunct condition, but the concerted late steps do not. Unexplained by this suggestion is the fact that the *Q-V* curve is less steep.

The three schemes drawn below represent the gating of a channel in three conditions: 1) normal gating, 2) gating of the channel in the dilated condition, and 3) gating charge movement of a defunct channel. Scheme 1 contains several early transitions followed by two late transitions, which are thought to be concerted and to precede the actual opening of the channel (Schoppa and Sigworth, 1998). Scheme 2 retains the early closed states from Scheme 1, but the kinetics of the late transitions are altered. In this scheme, the rightmost state (N) is nonconducting, and large-cation current flows when the channel is in the dilated (Dil) state. Finally, Scheme 3 corresponds to the gating of the defunct channels and has only early states, somewhat altered in behavior, as reflected in their broadened *Q-V* curve (Fig. 2). The conducting state and late closed states are inaccessible in defunct channels.

$$C_1 \underset{(0.3)}{\overset{6000}{\leftrightarrow}} \ldots C_m \underset{(0.3)}{\overset{7000}{\leftrightarrow}} C_n \underset{(0.52)}{\overset{(1.1)}{\leftrightarrow}} O \quad \begin{matrix} 340 & 240 \\ (0.18) & \end{matrix}$$

(Scheme 1, Normal condition)

$$C_1 \leftrightarrow \ldots C_m \underset{(0.3)}{\overset{\alpha_0 = 4000}{\leftrightarrow}} \text{Dil} \underset{(1.2)}{\overset{\rho_0 = 500}{\leftrightarrow}} \text{N} \quad \begin{matrix} (1.1) & (0.3) \\ \beta_0 = 25 & \zeta_0 = 0.17 \end{matrix}$$

(Scheme 2, Dilated condition)

$$C_{D1} \leftrightarrow \ldots C_{Dm}$$

(Scheme 3, Defunct condition)

Scheme 2 was used for the simulation shown in Fig. 5 *C*. The channels at 0 mV are mainly in the nonconducting state N. On stepping to very negative voltage, the channels mi-

grate from N to Dil and then on to the closed states $C_1 \ldots C_m$. The traces were empirically fit by selecting the best values at each voltage of the rate constants α, β, ρ, and ζ. These can be adequately summarized mathematically by the relations

$$\alpha = \alpha_0 \exp(z_\alpha \times V_m/kT) \qquad \beta = \beta_0 \exp(z_\beta \times V_m/kT)$$

$$\rho = \rho_0 \exp(z_\rho \times V_m/kT) \qquad \zeta = \zeta_0 \exp(z_\zeta \times V_m/kT)$$

where subscript 0 indicates the value at $V_m = 0$, z_i expresses the voltage dependence of each rate constant (given in parentheses in Scheme 2), and kT has the usual meaning. These equations and Scheme 2 were used to generate the curves in Fig. 5 *C*. One way of viewing these results is to say that the open state Dil is unstable because of its dilated conformation. Thus, at 0 mV, there is stability because state N is strongly favored, while at −140 mV or more negative, the stable closed states near C_1 are favored. But at voltages near −80 mV, the unstable state Dil is fairly probable, partly because the channels are unlikely to close, and its instability forces the channels into the defunct conformations represented by Scheme 3. When defunct, the central pore region of the channel (S5 and S6) is sufficiently deformed that the open state and the late closed states are rarely visited, although substantial S4 motion still occurs.

REFERENCES

Almers, W., and C. M. Armstrong. 1980. Survival of K permeability and gating currents in squid axons perfused with K^+-free media. *J. Gen. Physiol.* 75:61–78.

Chandler, W. K., and H. Meves. 1970. Sodium and potassium currents in squid axons perfused with fluoride solutions. *J. Physiol. (Lond.).* 211: 623–652.

Doyle, D. A., J. M. Carbal, R. A. Pfuetzner, A. Kuo, J. M. Gullbis, S. L. Cohen, B. T. Chait, and R. M. MacKinnon. 1998. The structure of the potassium channel: molecular basis of K^+ conduction and selectivity. *Science.* 280:69–77.

Gomez-Lagunas, F. 1997. *Shaker* B K^+ conductance in Na^+ solutions: a remarkably stable non-conducting state produced by membrane depolarizations. *J. Physiol. (Lond.).* 499:3–15.

Heginbotham, L., Z. Lu, T. Abramson, and R. MacKinnon. 1994. Mutations in the K^+ channel signature sequence. *Biophys. J.* 66:1061–1067.

Hoshi, T., W. N. Zagotta, and R. W. Aldrich. 1990. Biophysical and molecular mechanisms of *Shaker* potassium channel inactivation. *Science.* 250:533–538.

Jiang, Y., and R. MacKinnon. 2000. The barium site in a potassium channel by x-ray crystallography. *J. Gen. Physiol.* 115:269–272.

Jurman, M. E., L. M. Boland, L. Y. Liu, and G. Yellen. 1994. Visual identification of individual transfected cells for electrophysiology using antibody-coated beads. *BioTechniques.* 17:876–881.

Korn, S. J., and S. R. Ikeda. 1995. Permeation selectivity by competition in a delayed rectifier potassium channel. *Science.* 269:410–412.

Melishchuk, A., A. Loboda, and C. Armstrong. 1998. Loss of *Shaker* K channel conductance in 0 K^+ solutions: role of the voltage sensor. *Biophys. J.* 75:1828–1835.

Olcese, R., R. Latorre, L. Toro, F. Bezanilla, and E. Stefani. 1997. Correlation between charge movement and ionic current during slow inactivation in *Shaker* channels. *J. Gen. Physiol.* 110:579–589.

Perozo, E., R. MacKinnon, F. Bezanilla, and E. Stefani. 1993. Gating currents from a nonconducting mutant reveal open-closed conformations in *Shaker* K^+ channels. *Neuron.* 11:353–358.

Schoppa, N. E., and F. J. Sigworth. 1998. Activation of *Shaker* potassium channels. III. An activation gating model for wild-type and V2 mutant channels. *J. Gen. Physiol.* 111:313–342.

Starkus, J. G., L. Kuschel, M. D. Rayner, and S. H. Heinemann. 1998. Macroscopic Na^+ currents in the "nonconducting." *Shaker* potassium channel mutant W434F. *J. Gen. Physiol.* 112:85–93.

Starkus, J., L. Kuschel, M. Rayner, and S. Heinemann. 1997. Ion conduction through C-type inactivated *Shaker* channels. *J. Gen. Physiol.* 110: 539–550.